Electronic Supplementary Material (ESI) for Chemical Science.

Supporting Online Material for

Harnessing Isomerization-mediated Manipulation of Nonspecific Cell/matrix Interactions to Reversibly Trigger and Suspend Stem Cell Differentiation

Tao Bai[1], Andrew Sinclair[1], Fang Sun[1], Priyesh Jain[1], Hsiang-Chieh Hung[1], Peng Zhang[1], Jean-Rene Ella-Menye[1], Wenguang Liu[3], Shaoyi Jiang[1*]

[1]Department of Chemical Engineering, University of Washington, Seattle, WA 98195, USA

[2]School of Materials Science and Engineering, Tianjin Key Laboratory of Composite and Functional Materials, Tianjin University, Tianjin 300072 , P. R. China

*To whom correspondence should be addressed. Email: sjiang@uw.edu

Methods

Preparation of hMSC lysates. hMSCs at passage 3-4 were pelleted (1000 rpm, 4°C) and lysed into RIPA buffer (Sigma) which enables efficient cell lysis and protein solubilization while avoiding protein degradation and interference with the proteins' immunoreactivity and biological activity. The protein content of purified cell lysates was determined via BCA assay.

Preparation and purification of cRGD-functionalized CBAA monomer. As we reported before, Cyclo(RGDYKEG) peptide (cRGD) was functionalized to the system. In brief, appropriate amounts of N-(3-Dimethylaminopropyl)-N'-ethylcarbodiimide hydrochloride (EDC) (Sigma) and N-Hydroxysuccinimide (NHS) (Sigma) were added to CBAA monomer solution. After incubation at 25°C for 1 hour to activate the carboxylate group, an appropriate amount of cRGD was added to the activated system. The molar concentration of cRGD in the reaction solution was set at 150μM. The molar ratio of EDC, NHS and peptides was fixed at 1:1:1. The reaction was allowed to proceed at 25°C for 24 hours before purification. The efficiency of the reaction was calculated by LC-MS (Yield 78%).

An Agilent 1200 LC 6520 Q-Tof MS system (Agilent Technologies, Santa Clara, CA) was employed to purify the functionalized monomer and quantify the efficiency of the conjugation reaction. In brief, after the reaction, monomer sample was injected. The chromatographic separation was performed in hydrophilic interaction chromatography (HILIC) mode on a SeQuant ZIC-cHILIC column (150 x 2.1 mm, 3.0 μm particle size, Merck KGaA, Darmstadt, Germany). The flow rate was 0.500 mL/min, auto-sampler temperature was kept at 4°C, the column compartment was set at 40°C, and total separation time for both ionization modes was 40 min. The mobile phase was composed of Solvents A (5 mM ammonium acetate in 90% H_2O/10%

acetonitrile + 0.2% acetic acid) and B (5 mM ammonium acetate in 90% acetonitrile/10% H_2O + 0.2% acetic acid). The gradient conditions are shown below.

Time Segment, min.	Solvent A, %	Solvent B, %
0 – 1	25	75
1 - 5	from 25 to 70	from 75 to 30
5 - 9	70	30
9 – 9.1	from 70 to 25	from 30 to 75
9.1 – 40 (equilibration)	25	75

The Q-Tof mass spectrometer was equipped with an electrospray ionization (ESI) source. The instrument was controlled by an Agilent Mass Hunter Workstation (Agilent Technologies, Santa Clara, CA). The ESI voltage was set at 3800 volts. The source gas was N_2 (99.999% purity). The ion source conditions in positive mode were: drying gas = 10 L/min, nebulizer gas = 45 psi, temperature=325°C. The extracted ion chromatography (EIC, cRGD m/z=804.3602, cRGD-CBAA m/z=1015.5102,) peaks were integrated using Agilent Mass Hunter Qualitative Analysis software (Agilent Technologies, Santa Clara, CA). The functionalized monomers were purified by the LC system and obtained via lyophilization.

The functionalization efficiency was determined using $(V_c - V_f) / V_c \times 100$ (%), where V_f was the integrated value of the free cRGD after the reaction and V_c was the integrated value of the free cRGD in the aqueous solutions in which no coupling agents (EDC or NHS) were added.

Preparation of 3D hMSCs-PCB hydrogel constructs. An appropriate amount of CBAA, cRGD-functionalized CBAA, SPMA and CBDMA were dissolved in 40uL PBS. The molar concentration of CBAA, cRGD-functionalized CBAA, SPMA was fixed at 2M, 150mM, 10mM respectively and the molar concentration of crosslinker was adjusted to 20mM to produce hydrogels of desired mechanical rigidity.

For 3D cell-hydrogel constructs, cell/precursor solution (40μL) containing 6.1×10^7 cells ml^{-1} was used. Photoinitiator 2-hydroxy-2-methylpropiophenone was then added and mixed thoroughly to produce a final concentration of 0.05% (w/v). The solution was placed between two glass slides separated by 1.5 mm-thick polytetrafluoroethylene spacers and allowed to polymerize in a crosslink oven (XL-1500B UV Crosslinker, Spectronics Corporation, NY, USA) for 30s. The cell-encapsulating PCB hydrogels were equilibrated in basal media. During the first 5-hour equilibration, the basal media was refreshed every hour, and then refreshed every day. Visible and infrared light exposure was applied by employing customized MaxMax lighting system.

Viability assay. The viability of encapsulated cells was examined by using a LIVE/DEAD assay kit (Invitrogen). In order to remove the influence of cells on the surface of the gel, a 20 μm slice of the hydrogel from the surface was removed. Representative micrographs were acquired using a Zeiss LSM 510 META confocal microscope. At least three independent constructs were used. Three sections were sampled every 250-300 μm across the depth of the hydrogel and at least five different fields were randomly examined in each section. A Z-sampling rate of 2.1 μm was used for image acquisition.

Characterization of hydrogels. The hydrogels were obtained as described above and placed into PBS to reach equilibrium for at least five days before mechanical tests. At least five 0.5 cm diameter disks of each formulation (1.5 mm thickness when cast) were compressed at a rate of 1 mm/min using an Instron 5543A mechanical tester (Instron Corp., Norwood, MA) with a 10 kN load cell. The Young's modulus was calculated from 3% to 13% strain to avoid any complications in an instance in which the top plate may not be completely engaged with the specimen when compression begins.

The swelling ratios were determined using $(D_s/D_o) \times 100$ (%), where D_s was the diameter of the fully swollen hydrogels and D_o was the diameter of the relaxed (unswollen, but not dehydrated) hydrogels.

Preparation of self-assembled monolayers. Glass chips were first coated with an adhesion-promoting chromium layer (thickness 2 nm) and a surface-plasmon-active gold layer (48nm) by electron beam evaporation under vacuum. Before self-assembled monolayer (SAM) preparation, the gold-coated glass substrate was rinsed with ethanol and water in sequence, dried with filtered air, then further cleaned in a UV ozone cleaner (Jelight, model 42) for 20 min. The cleaned chip was immediately soaked in a 0.1 mM ethanol solution of ATRP initiator for 24 h to form a SAM on the gold surface[1]. The chip was subsequently rinsed with THF, then ethanol, and dried with a stream of filtered air just prior to surface-initiated polymerization.

Surface-initiated atom transfer radical polymerization. Surface-initiated ATRP was carried out on SAM-coated gold substrates following a method similar to one previously reported[1]. Briefly, CuBr, $CuBr_2$, BPY, and gold chips with immobilized initiators were placed in a sealed reaction tube and deoxygenated via vacuum and nitrogen purging. CBAA monomer was deoxygenated in a separate sealed tube, and then dissolved in a deoxygenated solution of methanol and pure water in a 10:1 volume ratio. The monomer solution was transferred to the reaction tube using a syringe under nitrogen protection. In a shaker at 120 RPM and 25°C, PCBAA was allowed to react for 3 h. After polymerization, chips were removed, rinsed with pure water and PBS, and stored overnight in PBS. Chips were rinsed with Milli-Q water and dried with filtered air just prior to any experiments. Dry film thickness was measured with an ellipsometer (J.A. Woollam, Alpha-SE), and chips with thicknesses of 20-30 nm were used for SPR measurements.

Measurements of protein adsorption: HMSCs lysates and FBS were used for the protein absorption assay. This study used a custom-built surface plasmon resonance (SPR) sensor from the Institute of Photonics and Electronics, Academy Sciences (Prague, Czech Republic). A prepared chip was attached to the base of the prism and optical contact was established using refractive index matching fluid (Cargille). A quadruple-channel flow cell with four independent parallel flow channels was used to contain liquid samples during experiments. A peristaltic pump (Ismatec) was utilized to deliver liquid samples to the four channels of the flow cell. A stable baseline was first established with PBS, then protein solution was delivered to the surface at a flow rate of 0.050 mL/min for 30 min, and finally the PBS was flowed again for 10 min before determining final wavelength shifts. A surface-sensitive SPR detector was used to monitor surface interactions in real time, and wavelength shift was used as an indication of changes on the surface.

Nonspecific protein adsorption on photodynamic hydrogels. After incubation with CLS or FBS, the hydrogel were rinsed with PBS before fluorescent detection. FluoroTag™ FITC Conjugation Kit (Sigma) and Rhodamine Conjugation Kit (Abcam) were used to label CLS and FBS as per manufacturer's instructions. Protein adsorption was detected by using Zeiss LSM 510 META confocal microscope. For all stacking images, a Z-sampling rate of 2.5μm was used for image acquisition.

Immunohistochemistry. After induced differentiation for 21 days, cell-hydrogel constructs were fixed in 4% paraformaldehyde in PBS for 8 hours, transferred to 30 wt% sucrose for 72 h, frozen in Cryo-gel (Instrumedics, Inc.) and cryosectioned (10μm sections). In order to remove the influence of the cells on the surface, a 20 μm slice of the hydrogel from the surface was removed. Vinculin-containing focal adhesion was stained by using ProteoExtract® Cytoskeleton

Enrichment and Isolation Kit (EMD Millipore) per the manufacture instruction. The F-actin filaments were stained with CytoPainter F-actin Staining Kit (Abcam) and mounted with ProLong Gold antifade reagent with DAPI and allowed to cure overnight.

Triple-label immunofluorescence staining was used to visualize differentiation markers and pluripotent markers. Mouse anti-RUNX2 (Abcam) and rabbit anti-OPN (Abcam) were used to visualize osteogenesis. Rabbit anti-PPARG (Abcam) and mouse anti-FABP4 (Abcam) were used to visualize adipogenesis. The cells were permeabilized for 10 minutes with PBT (0.1% Triton X-100 in PBS). After blocking for 1h in 10% fetal bovine serum, substrates were incubated with primary antibodies for 8 h at room temperature. Then, two types of secondary antibodies with different fluorescence tags, donkey anti-rabbit IgG (Invitrogen), and donkey anti-mouse IgG (Invitrogen), were used to visualize the antibodies of differentiation markers. 4,6-diamidino-2-phenylindole (DAPI; Molecular Probes) was included in the secondary solution and samples were mounted on glass slides with ProLong® Gold reagent. Representative micrographs were acquired using a Zeiss LSM 510 META confocal microscope. At least three independent constructs were used. Three sections were sampled every 250-300 μm across the depth of the hydrogel and at least five different fields were randomly examined in each section.

Quantitative Real Time PCR. At appropriate time points, constructs were removed from the culture media. Then, the constructs were transferred in TRI REAGENT (Sigma) in RNase-free test tubes and were homogenized with a tissue homogenizer. Total RNA was extracted according to the manufacturer's instructions. Total RNA for each sample was quantified with a UV spectrophotometer and converted to cDNA using the QuantiTect Reverse Transcription Kit. After amplification by using SYBR Green PCR Master mix (Qiagen), thermocycling was carried out in

a solution with primers (Integrated DNA Technologies) and cDNA. PCR conditions were as follows: 15s at 94 ºC, 30s at 55ºC, and 30s at 72ºC. The primer sequence is summarized in Supplementary Table S1[2-11]. Here, we used RNase-free DNase (Qiagen) to prevent genomic DNA contamination.

Osteogenic/Adipogenic Differentiation. Cell-hydrogel constructs were cultured in basal medium for 3 days. Following this time point, the basal medium was replaced with bipotential differentiation medium—low glucose DMEM supplemented with 20% FBS and 1% penicillin/streptomycin (Invitrogen); Adipogenic supplement: 1μM dexamethasone, 50μM indomethacin (Sigma), 0.5μM 3-isobutyl-1-methylxanthine (IBMX; Sigma) and 10μg/mL human recombinant insulin (Invitrogen); Osteogenic supplement: 10mM β-glycerol phosphate (Sigma), 50μg/mL ascorbic acid (Sigma). Media changes were performed every 3 days.

As a parallel control, a mixed adipogenic/osteogenic inductive media was made by combining commercially available osteogenic and adipogenic inductive media (R&D Systems) in a 1:1 ratio and supplementing with 1% (v/v) penicillin-streptomycin (Gibco). The mixed media was also used for the differentiation experiment mentioned above and no significant difference was observed compared to the lab-made bipotential differentiation medium.

Histological Analysis on hMSC differentiation. After incubation for 3 weeks, cell-hydrogel constructs were fixed in 4% paraformaldehyde in PBS for 8 hours, transferred to 30 wt% sucrose for 72 h, frozen in Cryo-gel (Instrumedics, Inc.) and cryosectioned (10μm sections). In order to remove the influence of the cells on the surface, a 20 μm slice of the hydrogel from the surface was removed. At least three independent constructs were used. Three sections were sampled every 250-300 μm across the depth of the hydrogel and at least five different fields were randomly

examined in each section. ALP activity (osteogenic biomarker) and neutral lipids (adipogenic biomarker) were visualized by Fast Blue BB (Sigma) and Oil Red O (Sigma). The total cell counts were obtained by staining the nuclei with DAPI. By dividing the positive stained cells for ALP and Oil Red O, respectively, by the total cell counts, the percentage of differentiated hMSCs proceeding through osteogenesis and adipogenesis was calculated. Color micrographs were acquired using a Nikon E800 upright microscope.

Inhibition assays. Inhibitors were added to cell culture media at the following concentrations without causing apparent changes to the viability of encapsulated hMSCs. Nocodazole (1.1μM), Cytochalasin D (0.25μM), Blebbistatin (1μM), and Y-27632 (1.8μM) (Calbiochem). Integrin blocking antibodies (α5 and β1, Chemicon) were added at 1.1ug/mL in the process of cell encapsulation.

Statistical analysis. Examination and quantification of histological sections was done by three independent researchers blinded to sample identity with at least five random images/fields in each section per sample. A two-tailed Student's *t*-test was used for all statistical analyses, with $*p<0.05$ being considered as statistically significant.

Synthesis of 1-(2-Hydroxyethyl)-2,3,3-trimethyl-3H-indolium bromide

A mixture of 2,3,3-trimethyl-3H-indole (25.0 g, 0.157 mol) and 2-bromoethanol (24.5 g, 0.196 mol) and acetonitrile (192 mL) were placed in a flask. The solution was heated at 90 °C for 24 h under nitrogen protection. After cooling down to ambient temperature, the solvent was evaporated under reduced pressure. The solid obtained was purified by solvent extraction with benzene for 24 h, and then dried overnight in vacuum. The product was further recrystallized from a mixed solvent of methanol (50 mL) and diethylether (150 mL) to obtain 1-(2-hydroxyethyl)-2,3,3-

trimethyl-3H-indolium bromide (32.8 g, 71.6 %) as pink solid. ^{1}H NMR (300 MHz, DMSO d6): d: 7.79 (m, 2H), 7.73 (m, 2H), 4.70 (t, 2H, J ¼ 8 Hz), 4.13 (t, 2H, J ¼ 8 Hz), 2.18 (s, 3H), 1.6 (s, 6H). ^{13}C (50 MHz, DMSO d6) d: 200.74, 144.4, 143.36, 132.48, 131.56, 126.1,117.74, 60.85, 57.4, 52.84, 24.69, 12.68.

Synthesis of 9,9,9a-trimethyl-2,3,9,9a-tetrahydro-oxazolo[3,2-a]indole. A solution of 1-(2-hydroxyethyl)-2,3,3-trimethyl-3H-indolium bromide (4.30 g, 15.90 mmol) and KOH (0.93g, 16.57mmol) in water (50 mL) was stirred at room temperature for 20 min. The product was extracted with ether and obtained under reduced pressure as yellow oil (Yield: 96.23%). 1H-NMR ($CDCl_3$): δ = 7.2-7.07 (m, 2H), 6.91 (t, 1H), 6.73 (d, 1H,), 3.79-3.62 (m, 2H), 3.53-3.46 (m, 2H), 1.38 (s, 3H), 1.34 (s, 3H), 1.18 (s, 3H). ^{13}C-NMR ($CDCl_3$): δ= 150.30, 139.76, 127.30, 122.23, 121.49, 111.75, 108.75, 62.77, 49.83, 46.72, 27.91, 15.08.

Synthesis of 1'-(2-Hydroxyethyl)-3',3'-dimethyl-6-nitrospiro(2H-1-benzopyran-2,2'-indoline). A solution of 2-hydroxy-5-nitorobenzaldehyde(25.0g,0.150mol) and 9,9,9a-trimethyl -2,3,9,9a- tetrahydro-oxazolo[3,2-a]indole (20.7 g, 0.102 mol) in ethanol (238 mL) was heated at 80°C for 16 h under nitrogen atmosphere. After cooling down to ambient temperature, the mixture was filtrated. The resulting solid was washed with ethanol (100mL) and dried to obtain the product as dark purple solid. ^{1}H NMR (300 MHz, CDCl3): δ 1.21 (3H, s), 1.31 (3H, s), 3.33-3.50 (2H, m), 3.71-3.82 (2H, m), 5.98 (1H, d), 6.68-7.22 (6H, m), 8.00-8.04 (2H, m). ^{13}C-NMR ($CDCl_3$): δ = 167.12, 159.29, 146.58, 141.09, 136.17, 135.44, 128.34, 127.91, 125.80, 122.71, 121.67, 119.84, 118.49, 115.41, 106.69, 106.37, 62.51, 52.67, 42.28, 29.57, 26.34, 25.77, 19.56, 18.38.

Synthesis of 1' -(2 -Methacryloyloxyethyl)-3',3' -dimethyl-6-nitrospiro(2H-1benzopyran-2,2'

-indoline) (SPMA). To a vigorously stirred solution of 2 (4.50 g, 12.8 mmol) and a catalytic amount of N,N-dimethylaminopyridine (0.22g, 1.8 mmol) in 50 mL CH_2Cl_2 at 0 ºC under an nitrogen atmosphere were simultaneously added CH_2Cl_2 solutions (each 20mL) of freshly distilled methacryolyl chloride (1.50 mL, 15.3 mmol) and triethylamine (2.14 mL, 15.3mmol) over a period of ca. 30 min. The reaction mixture was allowed to warm to room temperature overnight. The crude product was then subsequently washed with aqueous solution. The crude product in the organic phase was purified on a silica gel column using a hexanes/Ethyl acetate system. The purified product was further purified by recrystallization (hexanes; freezer) to give light yellow solid. Yield: 3.33 g (62%). crystals. Yield: 3.33 g (62%). ^{1}H NMR (300 MHz, $CDCl_3$): δ 8.00-7.88 (2H, m), 7.22 (1H, td,), 7.10 -7.08 (1H, dd), 6.93 -6.86 (2H, m), 6.78 -6.67 (2H, m), 6.08 (1H, m), 5.91 (1H, d), 5.58 (1H, m), 4.27 (2H, t), 3.60 -3.41 (2H, m), 1.93-1.90 (3H, m), 1.26 (3H, s), 1.19 (3H, s). ^{13}C NMR ($CDCl_3$): δ 166.9, 158.1, 146.2, 140.1, 135.8, 135.3, 128.2, 128.0, 126.0, 125.9, 122.4, 121.3, 120.0, 118.9, 115.3, 106.5, 106.3, 62.4, 52.1, 42.3, 25.5, 20.0, 18.2.

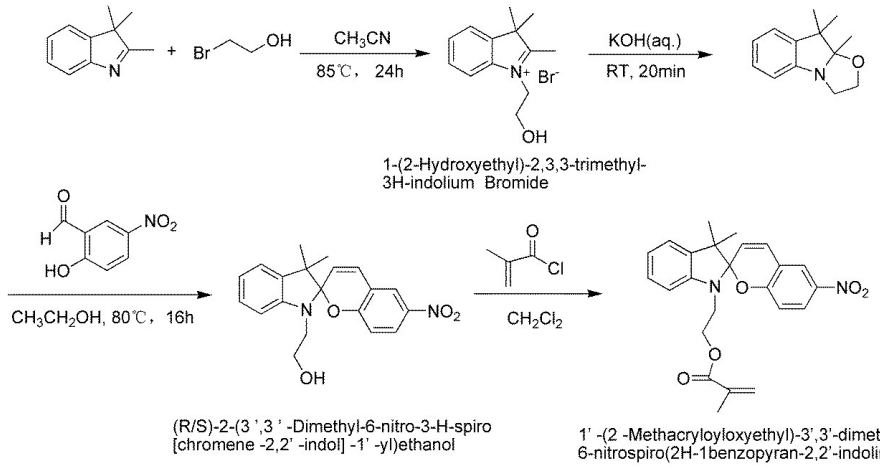

Supplementary Figure S1. Synthetic route of 1’ -(2 -Methacryloyloxyethyl)-3’,3’ -dimethyl-6-nitrospiro(2H-1benzopyran-2,2’-indoline) (SPMA).

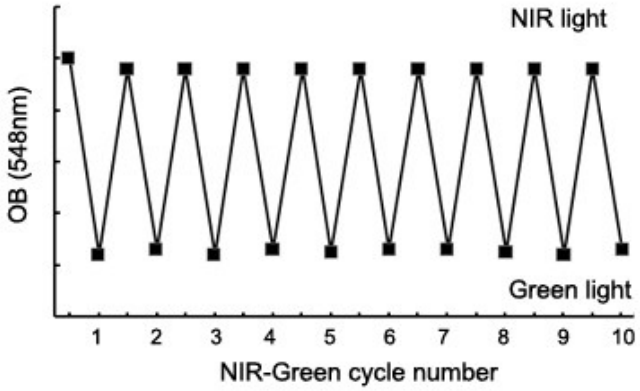

Supplementary Figure S2. Photoreversible switching (λ_{abs}=548nm) in this spiropyran-decorated zwitterionic hydrogel upon exposure to NIR and Green light.

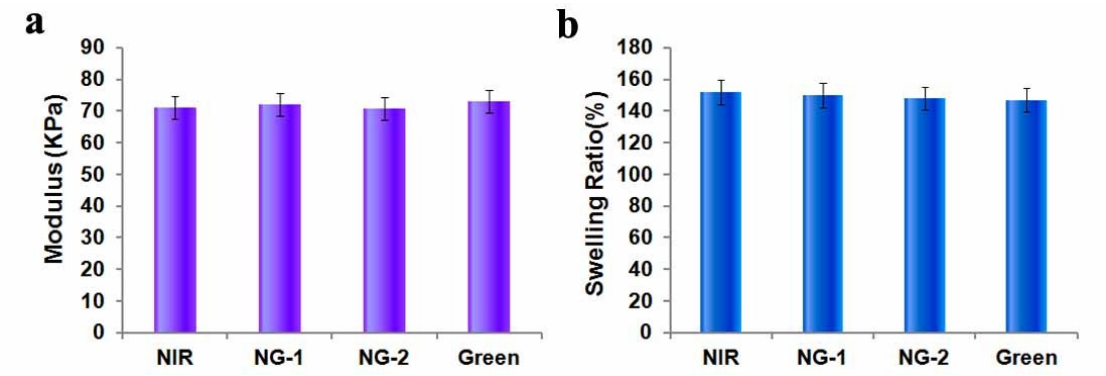

Supplementary Figure S3. Characterization of NIR, NG-1, NG-2 and Green hydrogels. **a)** Moduli of NIR, NG-1, NG-2 and Green hydrogels. **b)** Swelling ratios of NIR, NG-1, NG-2 and Green hydrogels.

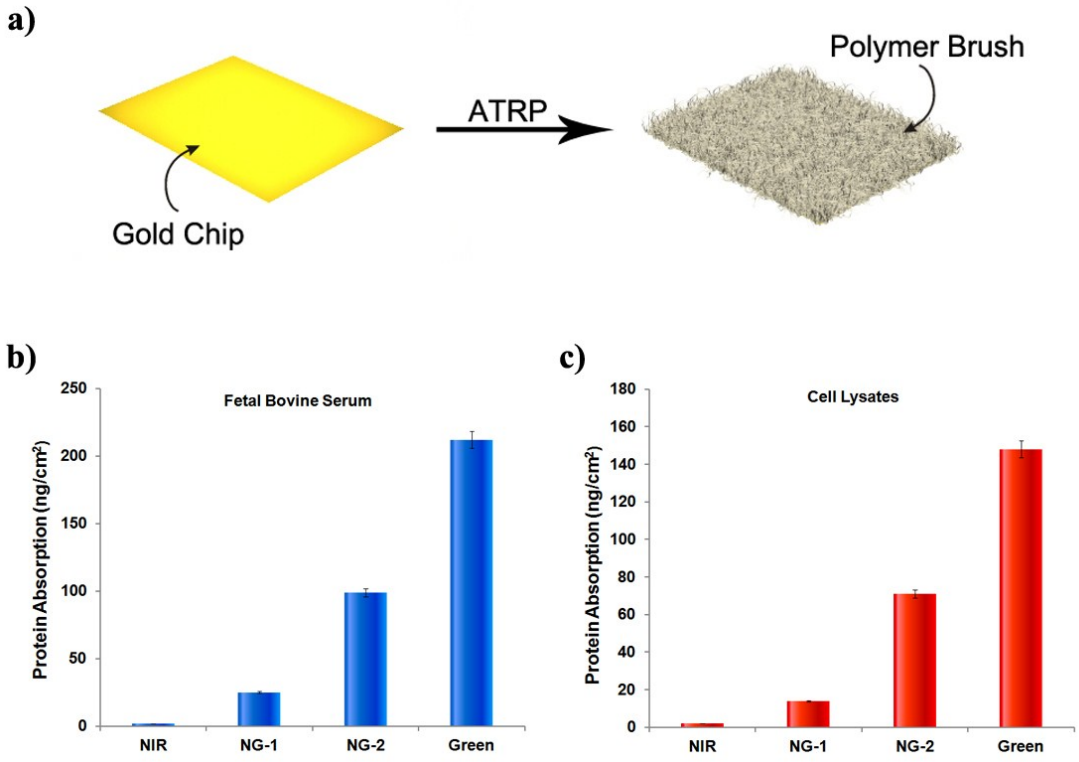

Supplementary Figure S4. a) Schematic illustration of grafting pSPMA polymer brush from gold chip by ATRP. **b-c)** Total protein adsorption was measured on an SPR sensor after injection of fetal bovine serum (FBS) and hMSCs lysates on pSPMA film receiving NIR, NG-1, NG-2 and Green light exposure.

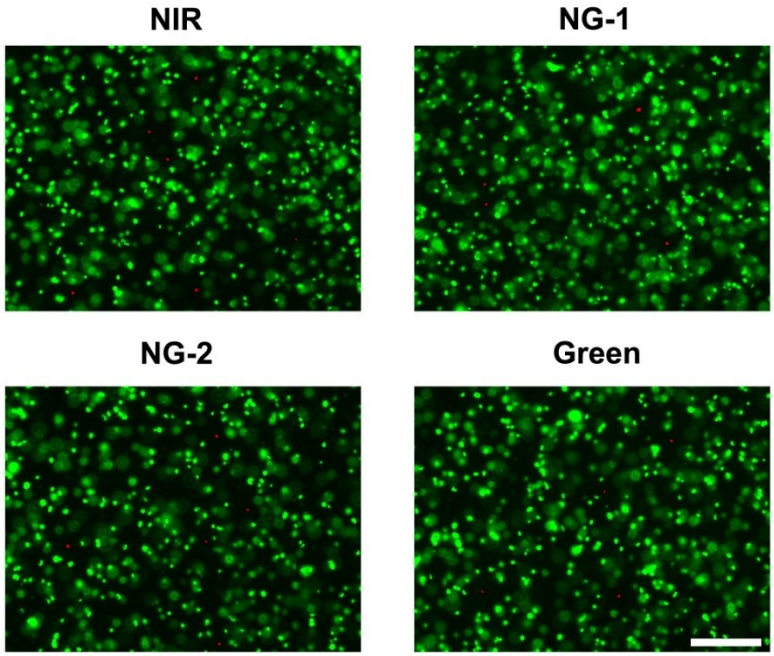

Supplementary Figure S5. LIVE-DEAD stain performed after encapsulating cells in NIR, NG-1, NG-2 and Green hydrogels after being cultured in bipotential medium for 14 days. Scale Bar: 200μm

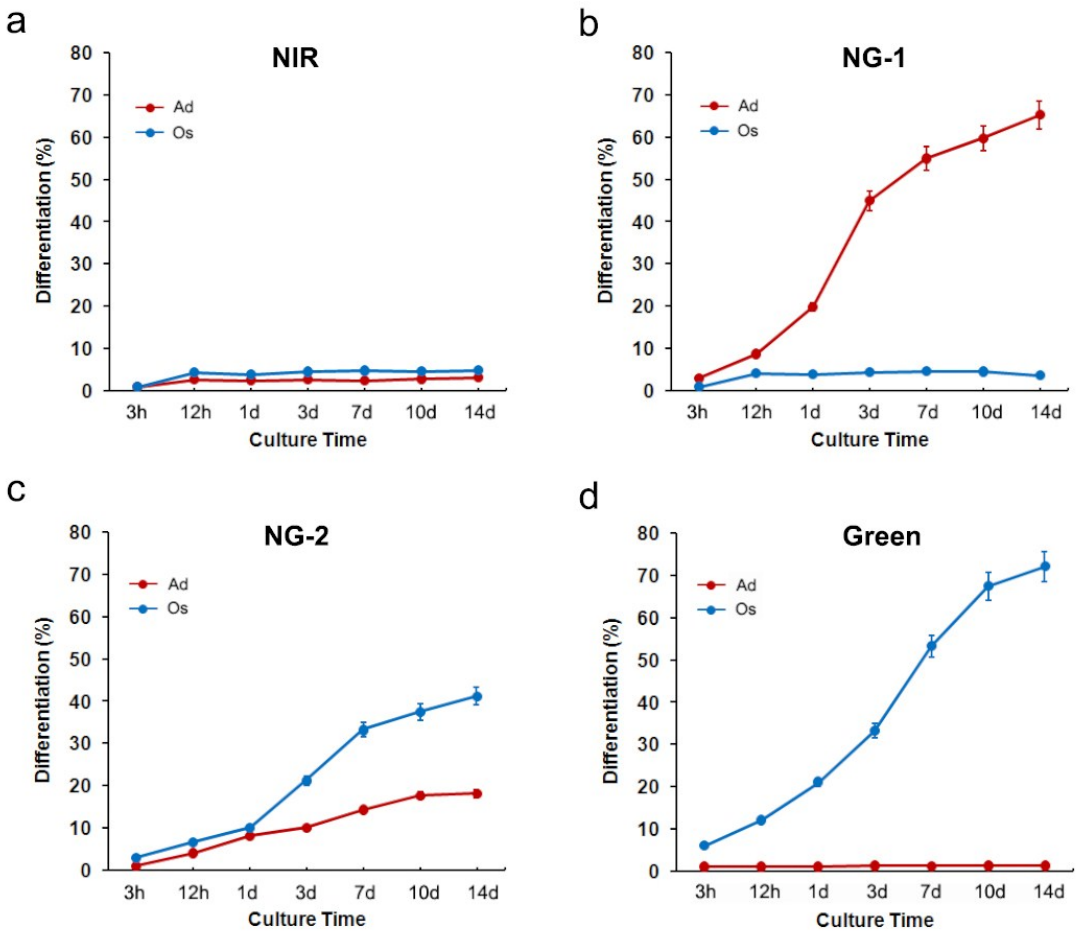

Supplementary Figure S6. Percentage change of cells expressing neutral lipids (red dots) and ALP (blue dots) under NIR (a), NG-1 (b), NG-2 (c) and green (d) illumination system.

qRT-PCR assessment of hMSC differentiation within 3D dynamic zwitterionic hydrogels. The expression of characteristic genes can accurately reveal the propensity of stem cells to differentiate. Thus, we next examined the behavior of stem cells within dynamic zwitterionic hydrogels at the RNA level. RNAs were isolated and we conducted quantitative real-time PCR (qRT-PCR) to test the expression levels of certain characteristic genes. Expression was normalized to cells at the time of encapsulation, with β-actin used as the housekeeping gene.

As exhibited in Supplementary Fig. S7a and e, hMSCs encapsulated in NIR hydrogels exhibited no enhanced expression of any of these differentiation marker genes. However, they presented noteworthy expression of adipogenic biomarkers (ADIPOQ, FABP4, LPL, PPARG) or osteogenic biomarkers (COL1A1, OCN, OPN, RUNX2) when green light was applied. Supplementary Fig. S7b-d summarizes the expression of a panel of adipogenic genes in hMSCs cultured in NG-1, NG-2 and Green hydrogels. As seen, all adipogenic genes were significantly upregulated in NG-1 hydrogel (a). However, their expression decreased sharply when stronger green light was applied (c-d). Supplementary Fig. S7f-h summarizes the expression of osteogenic genes by hMSCs in NG-1, NG-2 and Green hydrogels. Again, as seen, nonspecific-binding sites produced dramatic changes in the expression of osteogenic genes. As delineated in Supplementary Fig. S7f, compared to the negligible expression of osteogenic genes in NIR hydrogels, expression was hundreds of times higher in NG-2 and Green hydrogels. There were also significant differences when the concentration of nonspecific binding sites changed; stem cells in the photodynamic hydrogel with a weaker green light exposure expressed the osteogenic genes at a much lower level than those hydrogels received stronger green light exposure. The qRT-PCR results are consistent with our IHC and histology results.

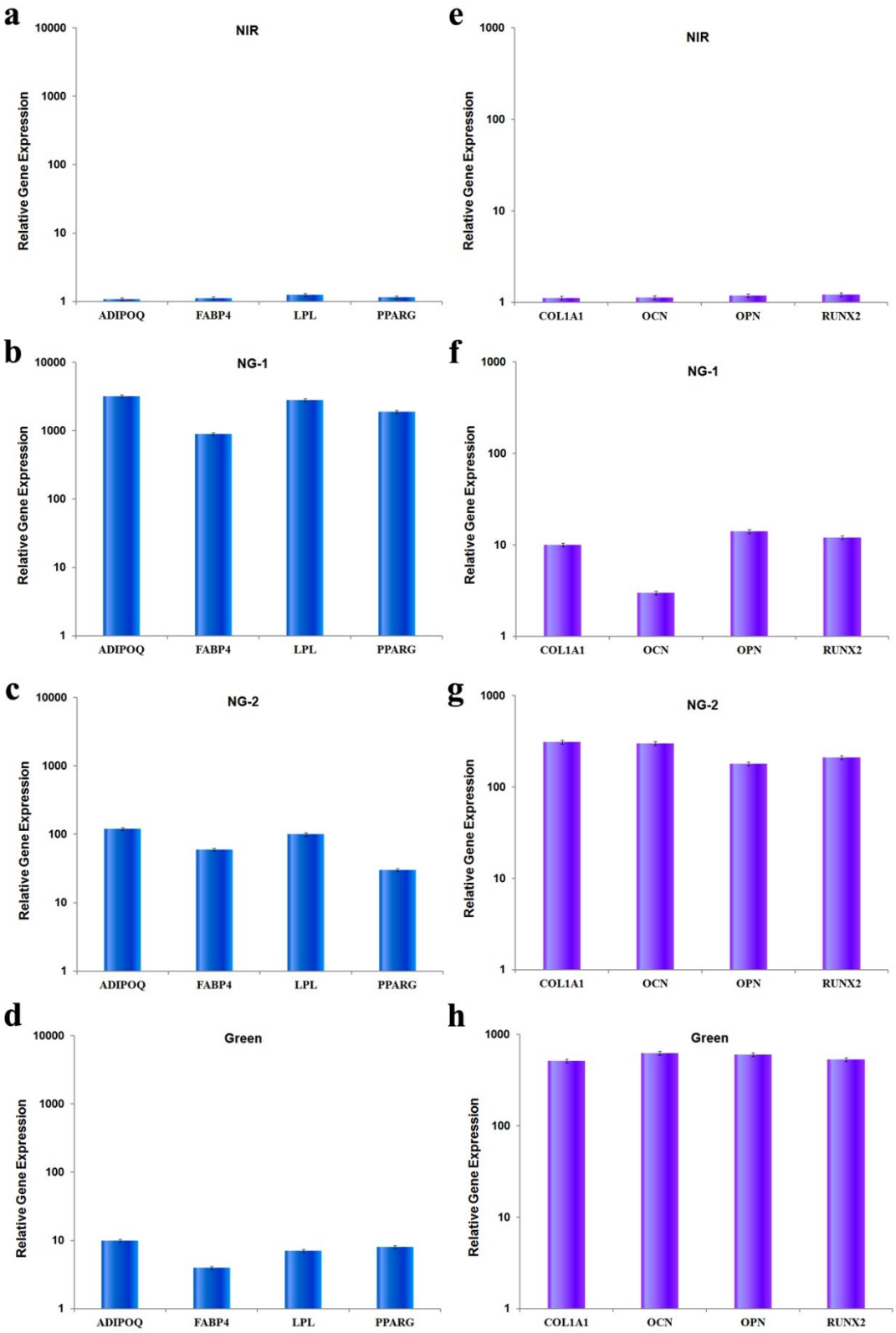

Supplementary Figure S7. Adipogenic (**a-d**) and osteogenic (**e-h**) gene activity of hMSCs cultured in photodynamic hydrogels receiving different light exposure in bipotential differentiation medium for 14 days. For all osteogenic and adipogenic genes, the percent expression was significantly different among NIR, NG-1, NG-2 and Green hydrogels (*$p<0.001$, t-test). Error bars represent standard error of the mean from 5 individual experiments.

Modulating differentiation by cytoskeletal manipulation. It has been reported previously that hMSC differentiation behavior depends directly on cytoskeletal contractility, which is highly related to the platform in which the cells reside. We thus assessed the influence of nonspecific interactions on the cytoskeletal contractility of encapsulated hMSCs. As in our previous report, nocodazole was added to the bipotential media to increase cell contractility, whereas blebbistatin, cytochalasin D, Y-27632 and antibodies against α5β1 integrin were supplemented to decrease cell contractility. None of these agents promote differentiation in the absence of nonspecific interactions under NIR exposure (Supplementary Fig. S8a). However, in the presence of nonspecific interactions under NG-1, NG-2 and green light exposure, hMSC differentiation preferences changed notably compared to the control group (Supplementary Fig. S8a). As presented in Supplementary Fig. S8b, when nocodazole interferes with microtubule polymerization and enhances cell contractility, encapsulated hMSCs present a clear preference for osteogenesis under all light conditions, notably reversing the adipogenic fate choice observed in the control group under NG-1 exposure. In addition, when the cell contractility was decreased by blebbistatin, cytochalasin D, Y-27632 and α5β1 antibodies, all encapsulated hMSCs under NG-1, NG-2 and green light presented a significant decrease in osteogenesis with a corresponding increase in adipogenesis (Supplementary Fig. S8c-f). It is further noted that the encapsulated hMSCs exhibited a higher differentiation rate when non-specific interaction was enhanced by stronger green light.

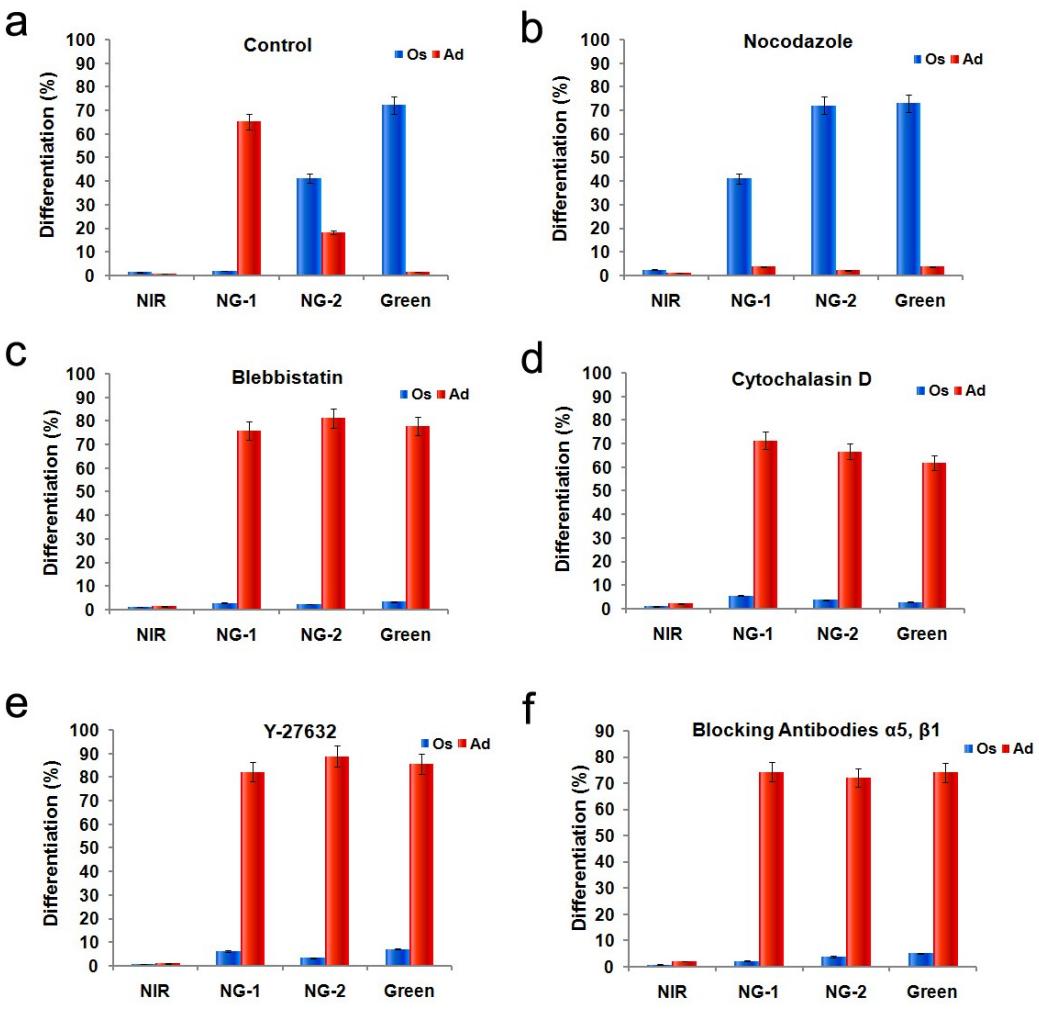

Supplementary Figure S8. Percentage of cells in hydrogels exposed to different light conditions differentiating to adipocytes (stained by Oil red O) or osteoblasts (stained by Fast Blue salt) in normal bipotential differentiation media (**a**) or in the presence of cytoskeleton disruptors and integrin blocking antibodies (**b-f**).

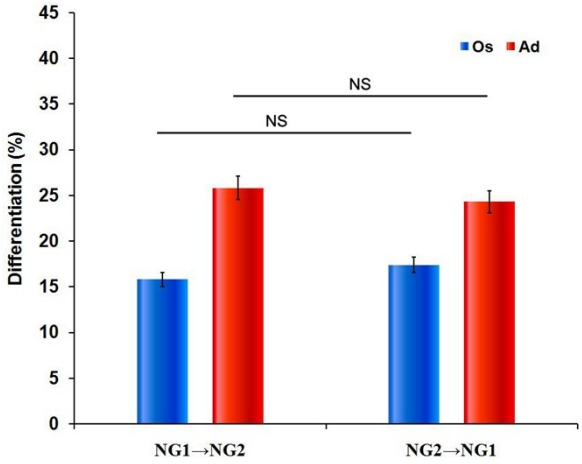

Supplementary Figure S9. Osteogenic and adipogenic differentiation rates of stem cells cultured on SP-decorated zwitterionic hydrogels exposed to 1-day NG1 illumination followed by 1-day NG2 illumination and hydrogels exposed to 1-day NG2 illumination followed by 1-day NG1 illumination. No significant difference was observed. Error bars indicate 95% confidence intervals. NS, not significant.

Table S1. Description of the primers sequence utilized for qRT-PCR.

Gene Symbol	Forward Primer	Reverse Primer
β3 TUBULIN	5'-GGCCTTTGGACATCTCTTCA	5'-CGGTCGGGATACTCCTCA
MYOD	5'-AGCACTACAGCGGCGACT	5'-GCGACTCAGAAGGCACGTC
AGGRECAN	5'-CACGCTACACCCTGGACTTG	5'-CCATCTCTCAGGAAGCAGT
RUNX2	5'-GATGACACTGCCACCTCTGA	5'-GACTGGCGGGGTGTAAGTAA
PPARG	5'-GCTGTTATGGGTGAAACTCTG	5'-ATAAGGTGGAGATGCAGGTTC
COL1A1	5'-TGAGAGACCAAGAACTG	5'-CCATCCAAACCACTGAAACC
OCN	5'-ATGAGAGCCCTCACACTCCTC	5'-CGTAGAAGCGCCGATAGGC
OPN	5'-CTAGGCATCACCTGTGCCATACC	5'-CAGTGACCAGTTCATCAGATTCATC
ADIPOQ	5'-CCTGGTGAGAAGGGTGAGAA	5'-CTCCTTTCCTGCCTTGGATT
FABP4	5'-GCCAGGAATTTGACGAAGTCAC	5'- TTCTGCACATGTACCAGGACAC
LPL	5'-GTGGCCGAGAGTGAGAACAT	5'-GAAGGAGTAGGTCTTATTTGTGGAA

Reference

1. Zhang, Z., Chen, S., Chang, Y. & Jiang, S. Surface grafted sulfobetaine polymers via atom transfer radical polymerization as superlow fouling coatings. *The Journal of Physical Chemistry B* **110**, 10799-10804 (2006).
2. Elmasri, H. et al. Fatty acid binding protein 4 is a target of VEGF and a regulator of cell proliferation in endothelial cells. *Faseb Journal* **23**, 3865-3873 (2009).
3. Jaiswal, R.K. et al. Adult human mesenchymal stem cell differentiation to the osteogenic or adipogenic lineage is regulated by mitogen-activated protein kinase. *Journal of Biological Chemistry* **275**, 9645-9652 (2000).
4. Khoo, M.L., Shen, B., Tao, H. & Ma, D.D. Long-term serial passage and neuronal differentiation capability of human bone marrow mesenchymal stem cells. *Stem cells and development* **17**, 883-896 (2008).
5. Lee, H.J. et al. Enhanced Chondrogenesis of Mesenchymal Stem Cells in Collagen Mimetic Peptide-Mediated Microenvironment. *Tissue Engineering Part A* **14**, 1843-1851 (2008).
6. Li, W.-J., Tuli, R., Huang, X., Laquerriere, P. & Tuan, R.S. Multilineage differentiation of human mesenchymal stem cells in a three-dimensional nanofibrous scaffold. *Biomaterials* **26**, 5158-5166 (2005).
7. Mwale, F. et al. The effect of glow discharge plasma surface modification of polymers on the osteogenic differentiation of committed human mesenchymal stem cells. *Biomaterials* **27**, 2258-2264 (2006).
8. Saussede-Aim, J. et al. Vinorelbine Induces beta 3-Tubulin Gene Expression through an AP-1 Site. *Anticancer Research* **29**, 3003-3009 (2009).
9. Sila-Asna, M., Bunyaratvej, A., Maeda, S., Kitaguchi, H. & Bunyaratavej, N. Osteoblast differentiation and bone formation gene expression in strontium-inducing bone marrow mesenchymal stem cell. *Kobe J Med Sci* **53**, 25-35 (2007).
10. Williams, C.G. et al. In vitro chondrogenesis of bone marrow-derived mesenchymal stem cells in a photopolymerizing hydrogel. *Tissue engineering* **9**, 679-688 (2003).
11. Zhang, F., Pomerantz, J.H., Sen, G., Palermo, A.T. & Blau, H.M. Active tissue-specific DNA demethylation conferred by somatic cell nuclei in stable heterokaryons. *Proceedings of the National Academy of Sciences* **104**, 4395-4400 (2007).